CHAPTER 3

Experimental procedure

This chapter contains the topics of the preparation and characterization of potassium sodium niobate ($K_{0.5}Na_{0.5}NbO_3$; KNN) glass ceramics by using incorporation method. The preparation steps of KNN glass ceramics include the powder preparation process, glass preparation process and crystallization process. Then, many characterization techniques of glass ceramic samples were introduced in order to investigate the glass and glass-ceramics samples, such as differential thermal analysis (DTA trace), Archimedes method, X-ray diffraction (XRD), Raman spectroscopy, field emission scanning electron microscope (FE-SEM), energy dispersive spectroscopy (EDS), UV-Vis-IR spectrophotometer, refractometer, ellipsometer and electrical determination as dielectric constant and losses.

In this work, the incorporation technique was used for the preparation of glass-ceramics due to the ability to control crystallization of the wanted single phase in the prepared glass matrices. This technique is very useful when compared to the conventional method, which always found unexpected secondary phases. Fig. 3.1 shows the different of the conventional glass-ceramic preparation and the incorporation method. In the conventional glass-ceramic preparation, all precursors as calculated from desired composition were mixed and melted before subjected to the heat treatment process for crystallization. In the incorporation method, the calcination or mixed-oxide technique was firstly introduced in order to synthesize the KNN single phase and then mixing with the glass former such as SiO_2 and TeO_2.

Next part, we will briefly describe the chemical compound and laboratory instrument lists in this work.

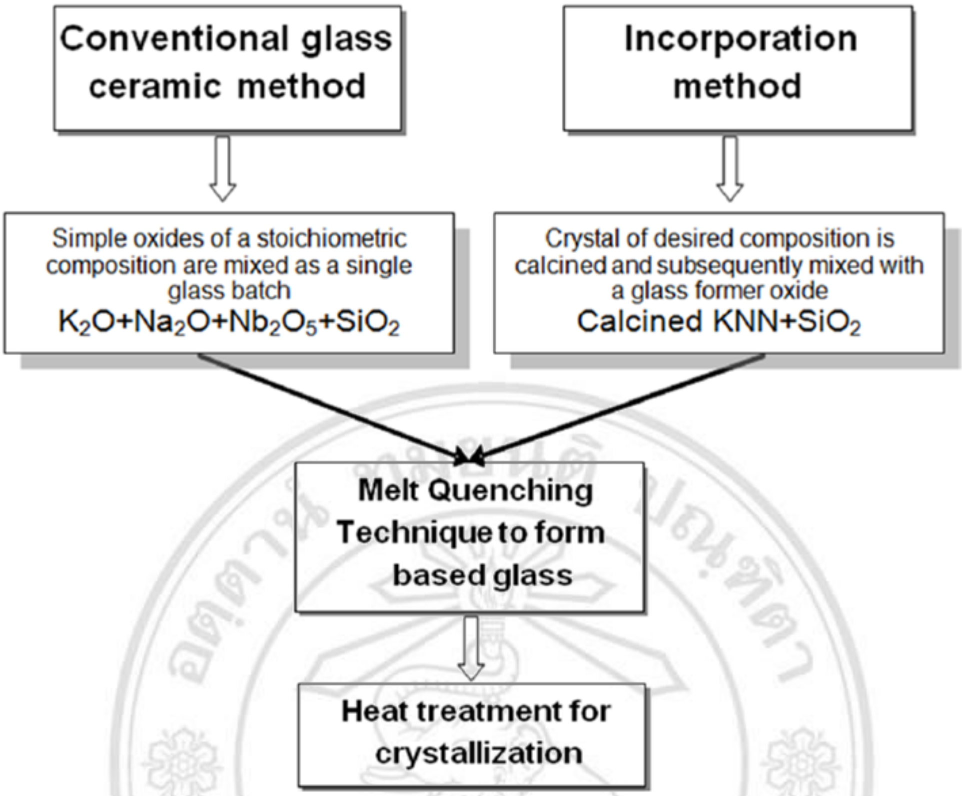

Figure 3.1 The diagram of conventional glass-ceramic method comparing with incorporation method [106].

3.1 Chemical reagents and laboratory instruments

3.1.1 Chemical reagent lists

1) Potassium carbonate (K_2CO_3), purity>99.0%, Sigma-Aldrich, Japan
2) Sodium carbonate, (Na_2CO_3), purity>99.8%, Sigma-Aldrich, Germany
3) Niobium (V) oxide (Nb_2O_5), purity>99.9%, Aldrich, Japan
4) Erbium (III) oxide (Er_2O_3), purity 99.9%, Aldrich, China
5) Aluminium oxide extra pure (Al_2O_3), Riedel-de Haen, Germany
6) Silicon dioxide (SiO_2), purity> 99.0%, Riedel-de Haen, Germany
7) Tellurium dioxide (TeO_2), purity>99.0%, Aldrich, Japan
8) Acetone (CH_3COCH_3), purity>99.5%, Duksan pure chemicals, Korea
9) Ethanol, (C_2H_5OH), purity>99.9%, MERCK

3.1.2 Laboratory instruments

1) Platinum Crucible
2) Stainless steel plate
3) Agate mortar
4) Electric furnace with maximum temperature of 1400-1700˚C
5) X-ray diffractometer (XRD, Rigaku, MiniFlex II, Japan)
6) Precision weighing balance (A&D, GR-200 series, Japan)
7) High temperature DTA cell adaptor (DTA, Du Pont Instrument, USA)
8) Raman spectroscopy (Jobin Yvon Horiba, T64000 series, monochrometor)
9) Field emission electron microscope (FE-SEM, JEOL, JSM 6335F type, Japan) with energy dispersive spectroscopy (EDS)
10) LCR meter (E4970A type, Agilent Technologies, Malaysia)
11) LCZ meter (E4980A type, Agilent Technologies, Malaysia)
12) Gold sputtering (JEOL, JFC-1100E series, Japan)
13) UV-Vis spectrophotometer (VARIAN Cary 50, USA; λ=190-1100 nm.)
14) Ellipsometer [J.A. Woollam Co., Inc. series α-SE^{TM}, USA]
15) Digital Refractometer (ABBE, D-22976 series, Hamburg)
16) Fluorescence Spectrometer (multichanel) (AvaSpec-2048TEC, Avantes, Netherlands) with Hg-lamp source (310-415 nm.) and laser emitting diode (980 nm.)

3.2 Sample preparation

3.2.1 Powder preparation

In this work, KNN powder was firstly prepared by solid-state oxide method. The calculated relevant proportions of $K_{0.5}Na_{0.5}NbO_3$ were weighed according to the formula below:

$$K_2CO_3 + Na_2CO_3 + 2Nb_2O_5 \rightarrow 4(K_{0.5}Na_{0.5})NbO_3 + 2CO_2 \qquad (3.1)$$

Generally, the single phase of KNN powder is rather difficult to prepare by conventional solid-state mixed oxide method, because the precursor as alkaline carbonate was highly sensitive to moisture and easily evaporate at high temperature, leading to the low possibility in forming the KNN single phase. Bomlai et al. [96] reported that an excess of 1, 3 and 5 mol% of Na_2CO_3 and K_2CO_3 with ratio 1:1 resulted in the ease of formation of KNN single phase. We therefore have chosen to prepare KNN powder with an excess of 5 mol% Na_2CO_3 and K_2CO_3 (ratio 1:1). Finally, single phase KNN was successfully prepared by excess 5 mol% of K_2CO_3 and Na_2CO_3 at the calcinations state. All commercial starting powders were weighted as listed in Table 3.1, for preparing KNN powder.

Table 3.1 Nominal composition of the starting powders used in this study.

Powder	**Weight (g)**	
	50	**100**
Na_2CO_3	8.0900	16.1800
K_2CO_3	10.5500	21.1000
Nb_2O_5	38.6450	77.2900
Total	57.2850	114.5700

The starting materials were mixed by a ball milling technique for 24 h. in a polyethylene bottle by using zirconia balls and acetone as grinding and liquid media respectively. Well mixed powder was dried by using a magnetic stirring hot plate at 40-60˚C for 24 h. and the sample was kept in an oven for 24 h. at the same temperature. Then, the dried powder was calcined in an electric furnace at 900˚C for 5 h. with a heating rate and a cooling rate of 1.67˚C/min and 5˚C/min, respectively. The obtained KNN powder was agglomerated, therefore, it is necessary to sieve the obtained powder. The overview of powder preparation process was shown in Fig. 3.2.

To examine some properties of this KNN powder, XRD, FE-SEM and EDS were employed. The results are shown in Fig. 3.3, 3.4 and Table 3.2, respectively. From the observation, KNN single phase was successfully prepared by excess Na_2CO_3 and K_2CO_3 of about 5 mol%.

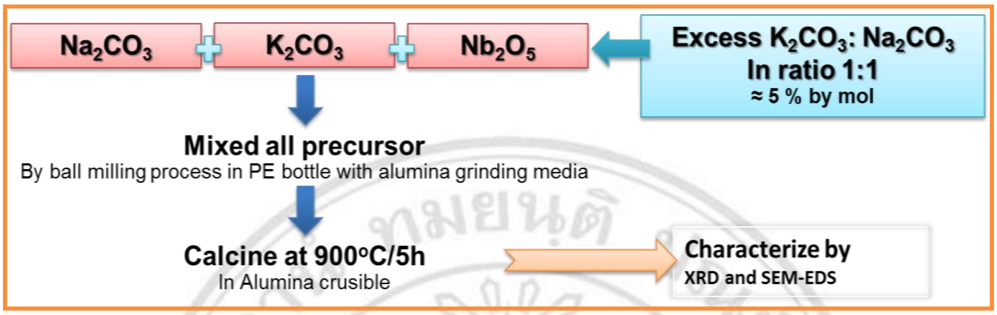

Figure 3.2 Schematic diagram of powder preparation process.

Phase formation of the calcined KNN powders was examined by X-ray diffraction (XRD) technique. Scanning electron microscope (FESEM-EDS) was used to investigate phase morphology. Results of phase formation and morphology of KNN powders are given as follows.

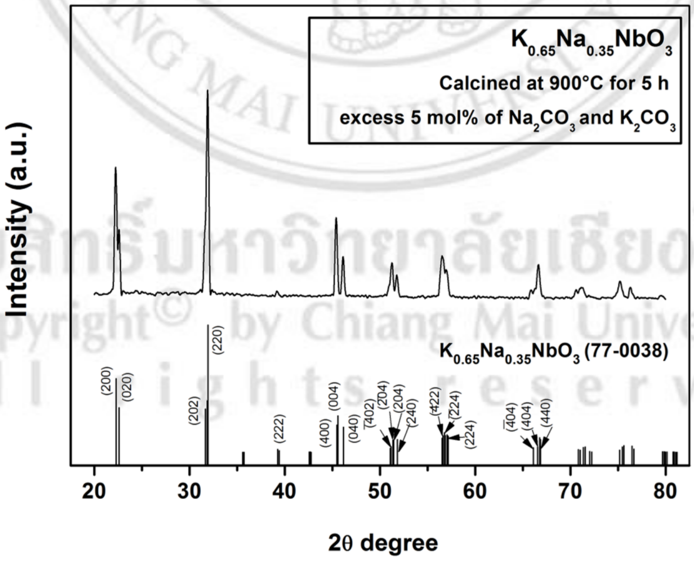

Figure 3.3 X-ray diffraction patterns of KNN with 5 mol% of Na_2CO_3 and K_2CO_3 in ratio 1:1 and calcined at 900°C for 5 h ($K_{0.5}Na_{0.5}NbO_3$ phase).

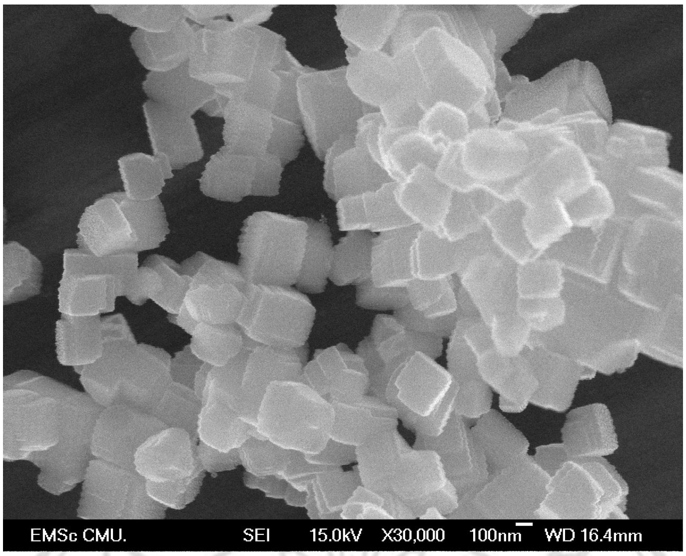

Figure 3.4 The SEM image of KNN powder obtained cubic crystal sizes 100-200 nm at 900 °C for 5 hours [106].

Table 3.2 Quantitative analysis of calcined KNN powder at 900 °C for 5 hours by EDS technique [106].

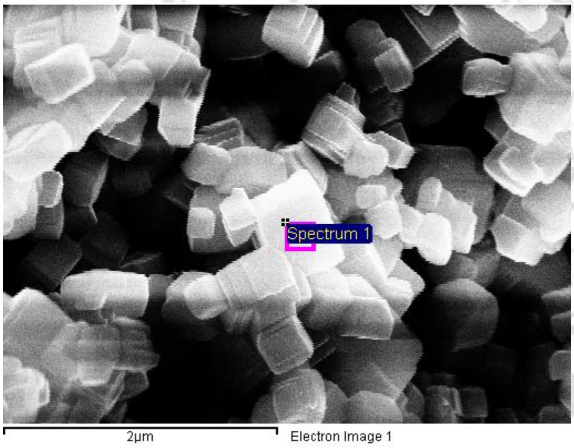

Element	Weight%	Atomic%
O K	41.35	72.88
Na K	6.14	7.53
K K	8.73	6.30
Nb L	43.78	13.29
Totals	100.00	

From Fig. 3.3, it is clearly seen that the KNN single phase can be achieved by the excess of 5 mol% Na_2CO_3 and K_2CO_3. To confirm single phase, data was compared with JCPDS file number 77-0038 [Appendix A].

It can be assumed that by using stoichiometric compositions of Na_2CO_3, K_2CO_3 and Nb_2O_5 to prepare the KNN powder, the incomplete reaction via calcination method is likely to occur because of the compositional fluctuation from easily volatile precursors such as Na_2CO_3 and K_2CO_3 at high temperature. The FE-SEM micrograph in Fig. 3.4 shows the morphology of the prepared KNN crystals with cubic shape and size ranging from 100 nanometers to 2 micrometers. The EDS study (Table 3.2) also confirms the composition of the prepared powder which has the weight and atomic ratio of Na:K close to 1:1 as expected.

3.2.2 Glass preparation

After successfully prepared KNN single phase powder, the KNN powders were mixed with the glass forming reagent as SiO_2 or TeO_2 in various compositions to form transparent glass ceramics. Glass composition of one batch was shown in Table 3.3.

Glass forming substance and KNN powder were mixed (Fig. 3.5) and melted in platinum crucible via electric furnace (Fig. 3.6) at melting temperature (T_m), (T_m of TeO_2 = 800˚C and T_m of SiO_2 = 1300˚C) and subsequently quenched between stainless steel plates (Fig. 3.7) near glass transition temperature (T_g) to avoid the internal stress cracking. The as-received glass was then annealed for 6 h to release their stress. The T_g of each glass was studied by DTA technique in order to find the optimize annealing temperature and T_g. DTA technique also gives the thermal information such as T_c (crystallization temperature) and T_m. Fig. 3.8 and 3.9 shows the overview of glass preparation process of 2 based glass systems.

Figure 3.5 Platinum crucible.

Table 3.3 Chemical compositions of the prepared glass samples.

Glass composition	Weight (gram unit)				Total (g)
	KNN	TeO_2	SiO_2	Er_2O_3	
30KNN-70TeO_2	4.7310	10.2690	-	-	15
20KNN-80TeO_2	3.1770	11.8230	-	-	15
30KNN-70TeO_2 doped 0.5 Er_2O_3	4.6755	10.1505	-	0.1740	15
30KNN-70TeO_2 doped 1.0 Er_2O_3	4.6215	10.0320	-	0.3465	15
20KNN-80TeO_2 doped 0.5 Er_2O_3	3.1395	11.6850	-	0.1755	15
20KNN-80TeO_2 doped 1.0 Er_2O_3	3.1035	11.5485	-	0.3480	15
70KNN-30SiO_2	13.0462	-	1.9538	-	15
75KNN-25SiO_2	13.4351	-	1.5649	-	15
80KNN-20SiO_2	13.7949	-	1.2051	-	15
70KNN-30SiO_2 doped 0.5 Er_2O_3	12.8675	-	1.9270	0.2055	15
70KNN-30SiO_2 doped 1.0 Er_2O_3	12.6919	-	1.9007	0.4074	15
75KNN-25SiO_2 doped 0.5 Er_2O_3	13.2581	-	1.5443	0.1976	15
75KNN-25SiO_2 doped 1.0 Er_2O_3	13.0840	-	1.5240	0.3920	15
80KNN-20SiO_2 doped 0.5 Er_2O_3	13.6199	-	1.1898	0.1903	15
80KNN-20SiO_2 doped 1.0 Er_2O_3	13.4475	-	1.1748	0.3777	15

*Maximum melted is 15 g/batch

Figure 3.6 Electric furnace.

Figure 3.7 Stainless steel plates.

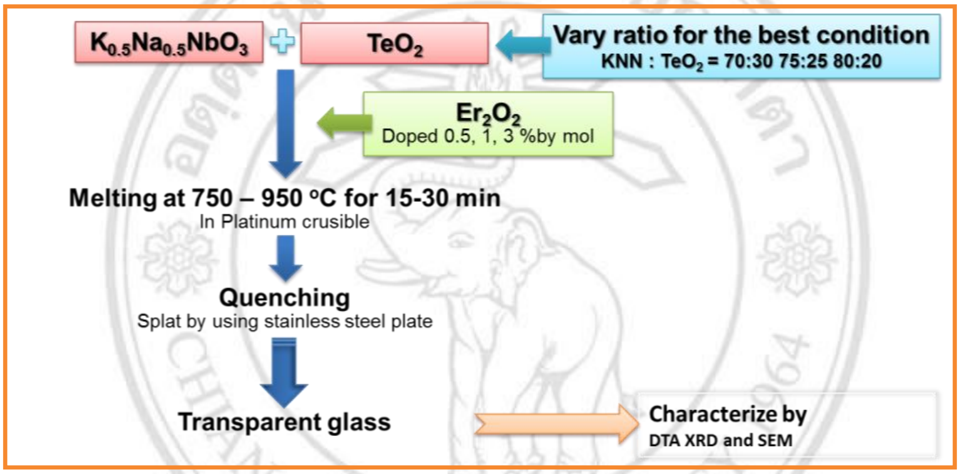

Figure 3.8 Schematic diagram of KNN based TeO_2 glass preparation process.

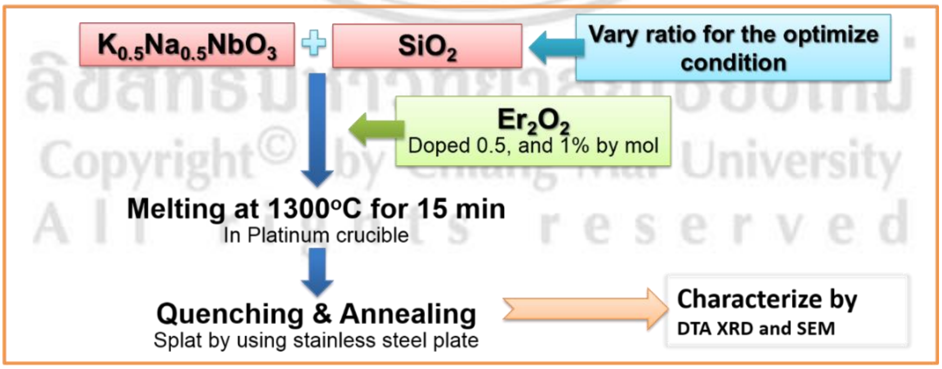

Figure 3.9 Schematic diagram of KNN based SiO_2 glass preparation process.

3.2.3 Crystallization process

In this step, as-received glass was subjected to grow KNN crystals via heat treatment (HT) technique depending upon the T_g and T_c of each glass (ranging from 300 to 550 °C) for 2-6 h with heating rate of 5°C/min and cooling rate of 10°C/min to form the desired crystal of KNN phase. These crystallization temperatures were determined from the DTA trace resulted of the as-quenched glass as mention above. Fig. 3.10 shows the overview of glass ceramics preparation process.

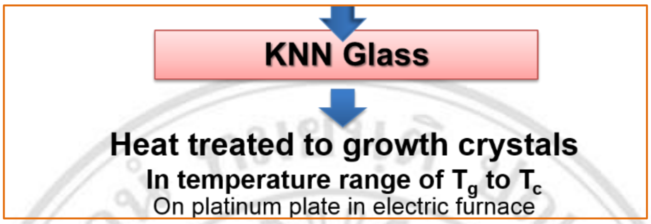

Figure 3.10 Schematic diagram of crystallization process for glass ceramics.

3.3 Glass ceramics characterization

The density of glass and glass-ceramic samples could be calculated from Archimedes method. The thermal property of each glass system was studied by DTA analysis. The XRD and SEM techniques were used for investigation of the phase formation and the microstructure of each sample. The optical transmission spectra and refractive index were measured using an UV-VIS-NIR spectrometer, refractometer and Ellipsometer. The photoluminescence was measured by fluorescence spectrometer with two excitation sources; laser emitting diode at 980 nm and Hg-lamp source of about 310-415 nm. Glass-ceramics were polished in 2 parallel surfaces. Then, sputtering technique was used for gold coated in order to create the electrical contact. The dielectric constant (ε_r) and dielectric loss (tanδ) were measured at various frequencies, ranging from 10 kHz to 1 MHz by precision LCR and LCZ meter.

3.3.1 Thermal analysis

In general, the thermal property was studied via three different experimental techniques, such as thermogravimetric analysis (TGA), differential thermal analysis (DTA) and differential scanning calorimetry (DSC). In this studied, DTA (Fig. 3.11) is only one technique used for determine the glass transition temperatures, crystallization temperatures and melting temperatures (T_m). To prepare sample for DTA measurement, as-received glass were ground into fine powder and placed in to small alumina crucible by using highly pure silica and alumina as reference materials for tellurite and silicate glass-ceramic systems. The weight per batch is 0.05 g. The temperature range in this study is 30-900°C with heating rate of 5°C/min.

The DTA technique does not measure the mass changes of sample. The DTA working by measuring the difference of temperature between an inert reference and the ground glass sample. The change of temperature between the inert reference and the glass sample is detected by DTA signal, which means, there are some transformation in a physical or chemical properties. This technique is usually applied in many studies such as the identification, the analysis of quantitative composition, the phase formation diagrams, the hydration and dehydration, the thermal stability, the polymerization, purity, and reactivity.

Figure 3.11 Differential thermal analyzer, DTA.

3.3.2 Densification analysis

The bulk density was determined for all glass and glass-ceramic samples, the weight was measured using a precision weighting balance with density equipment (Fig. 3.12). The bulk density (ρ_b) was calculated using Archimedes' principle according to the equation (3.2):

$$\rho_b = \frac{W_D}{V_b} \tag{3.2}$$

where W_D is the dry weight of specimen and V_b is the bulk volume.

The density (ρ) of the immersed object relative to the density of the fluid (ρ_{Fluid}) at room temperature (T_r) can be easily calculated without measuring any volumes:

$$\rho = \frac{W_{Air}}{W_{Air} - W_{Fluid}} \bullet \rho_{Fluid}\left(T_r\right) \tag{3.3}$$

Where W_{Air} is the weight in air of the specimen and W_{Fluid} is the weight in fluid of the specimen. In this research, the glass and glass-ceramic samples were measured with distilled water as the immersion liquid (fluid).

Figure 3.12 Precision weighing balance.

3.3.3 Phase analysis

1) X-ray diffractometer

X-ray diffraction (Fig. 3.13) analysis was conducted to determine the $(K_{0.5}Na_{0.5})NbO_3$ single phase powder obtained from calcination process and $(K_{0.5}Na_{0.5})NbO_3$ crystalline phase formation within glass-ceramics materials. All $(K_{0.5}Na_{0.5})NbO_3$ glass and glass-ceramic samples were ground into fine powders, placed in the holder of a diffractometer and scanned with CuKα radiation, 1.5418 Å, λ at 40 kV and 15 mA. In addition, diffraction patterns were collected in the 2theta (2θ) ranging from 20° to 80° with step size of 0.02° per second. The diffraction patterns were matched with the Joint Committee of Powder Diffraction Standard (JCPDS) database, for determining phase existed in the samples.

The crystallite size was estimated using the Scherrer equation: [97]

$$d = \frac{k\lambda}{\beta_{crystalline} \cos\theta} \tag{3.4}$$

where $\beta_{crystalline}$ is the full width at half maximum (FWHM), obtained for high intense peak, in the present studies), k is a constant which is usually varies in the range from 0.89 to 1.00, depending on the crystalline shape, in this study $k = 0.9$, λ is the wavelength used (1.5406 Å), d parameter is the average of crystallite size measured in a direction that perpendicular to the specimen surface and θ is stead of Bragg angle.

2) Raman Spectroscopy

In achievement of network structure information of amorphous and crystalline phase of erbium doped sodium potassium niobate, Raman spectroscopy (Fig. 3.14) has taken an advantage in structural determination. Glass samples were grounded in to fine powder. Then, the samples were placed on a glass slide in order to characterize the response of molecules to energy. Raman scattering data was collected by a microscope equipped with 100x lenses using 532 nm exciting light of solid state laser operating at 50 mW. The acquisition time required for the recording of each spectrum was 120 seconds.

3) Fourier transform infrared spectroscopy

Fourier spectroscopy is the analysis of the component frequency of each matter. Fourier transform infrared spectroscopy or FT-IR have various mode such as the absorption, reflection, emission, or photo-acoustic spectrum mode, which are useful for using in long range of frequencies from ultraviolet, visible, near infrared, mid infrared and far infrared regions by selecting different beam splitters and detectors for the required ranges.

The infrared spectroscopy worked by releasing the IR radiation to the samples and collected the IR radiation that transmitted the samples. The obtained spectrum exhibits the absorption and transmission of molecules, which generate a fingerprint of molecular structure ofsample. This advantage makes the infrared spectroscopy useful for several types of analysis. To prepare the sample for FT-IR analysis, fine glass-ceramic powders were placed in FT-IR holder by carefully avoiding moisture problem. The schematic diagram of FT-IR spectrometer is shown in Fig. 3.15.

Figure 3.13 X-ray diffractometer.

Figure 3.14 Raman spectrometer.

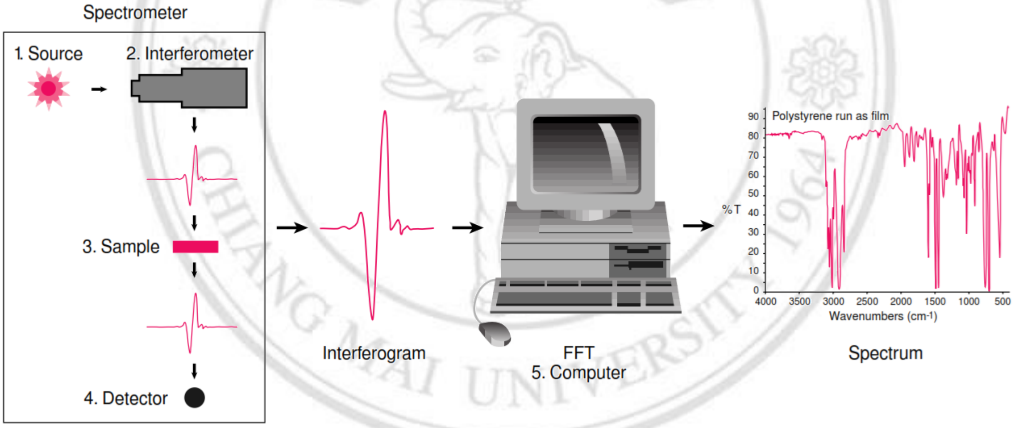

Figure 3.15 FT-IR spectroscopy operating system [98].

3.3.4 Microstructural analysis

In this research, cross-sectional glass and glass-ceramic samples were polished and some samples were etched with 1 mol % of hydrofluoric acid (HF) for 2 min to create surface profile. Well prepared samples were attached to copper stub by carbon tapes and then coated with gold (Au) by sputtering technique with 2 MPa for 10 sec. All of the processes must be avoided from the environment moisture. The SEM study is the field emission type equipped with an energy dispersive X-ray analyzer (EDX) (Fig. 3.16). The chemical composition of the significant microstructural features was also analyzed using an EDX technique.

Figure 3.16 SEM-EDS spectroscopy.

3.3.5 Measurement of optical properties

1) Transmittance (%) and absorbance

In this research, the glass and glass-ceramic samples were polished to optical quality on both surfaces in order to obtain a sample thickness of 1 mm. The optical transmission spectra were measured using an ultraviolet-visible-near infrared (UV-Vis-NIR) spectrophotometer (Fig 3.16) in the range of 200 to 1200 nm.

The spectrophotometer detected the light that transmitted from the sample. This transmitting light wavelength is not the same wavelength compared to the light source due to the light absorption in material. The detector of spectrophotometer is sensitive to transmitted light. The reference solution was counted on a blank which contains no analysts, but sometime contain the reagents that are intentionally added to the sample. The spectrophotometer compares the interaction of light in the sample and the blank in order to demonstrate the effect of the analyst. The transmittance is estimated as shown in equation (3.5) [49]:

$$\frac{Transmitted\ light\ from\ sample}{Transmitted\ light\ from\ the\ blank} = Transmittance\ (t) \qquad (3.5)$$

and percent transmittance is:

$$\%T \quad = \quad t \times 100\ \% \qquad (3.6)$$

The transmittance or percent transmittance can be ranging from 0 or 0% (100% light absorbed in sample or no light transmitted) to 1 or 100% (0% light absorbed in sample or all light passes through). In general, the spectrophotometers frequently measure the transmittance which is estimated from equation (3.5), however, analysts are usually interested in the absorption of light in a sample. Therefore, there are an additionally way to convert transmittance to a measure of light absorption as called absorbance. Absorbance can be calculated by using the transmittance as shown in equation (3.7):

$$A \quad = \quad -\log\ (Transmittance) \qquad (3.7)$$

The absorbance is sometimes called the optical density or OD. With modern spectrophotometers, you can adjust the instrument to either read out transmittance or to automatically convert the reading to an absorbance value. The UV-Vis-IR spectrophotometer is shown in Fig. 3.17.

Figure 3.17 UV-Vis-NIR spectrophotometer.

2) Refractive index

In general, when light pass through the medium, the speed of light is usually decreased. There is a significant value called refractive index or index of refraction (*n*) that used to explain the term of light speed in each medium. For example, the glass that used in daily life as soda-lime system has *n* = 1.5, which means that in glass, light travels at 1/1.5 or 0.67 times the speed of light in a vacuum. This value is very important for glass materials or other transparent materials because this value is related to the two important properties as, the change of light ray direction when it pass through the air to material at the interface (Fig. 3.18) and the partially reflection of light from surface in which the refractive index is different from nearest surroundings.

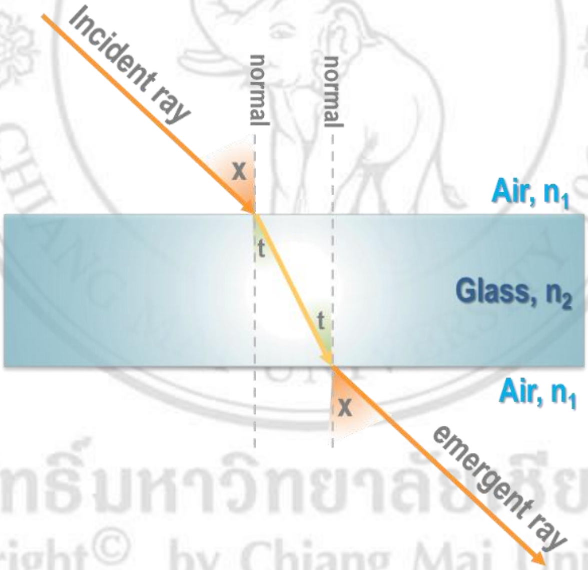

Figure 3.18 Schematic diagram of refraction by light from air to glass to air.

The refractive index (*n*) of a medium is defined as the ratio of the phase velocity (*c*) of a wave phenomenon such as light or sound in a reference medium to the phase velocity (ν_p), in the medium itself as shown in equation 3.8.

$$n = \frac{c}{\nu_p} \tag{3.8}$$

The vacuum is commonly used in the context of light as a reference medium even if there are many other reference media as air at pressure and temperature standard as related to equation 3.9.

$$n = \sqrt{\varepsilon_r \; \mu_r} \tag{3.9}$$

where ε_r is the relative permittivity of sample and μ_r is its relative permeability. The μ_r of most materials showed very close to 1 at optical frequencies. Hence, *n* is approximately $\sqrt{\varepsilon_r}$ [100].

Here, in this research, the refractive index of glass-ceramics was studied by 2 analytical instruments refractometer (Fig. 3.19) and ellipsometer (Fig. 3.20), which have the difference theoretical analysis.

2.1) Reflectometry

Reflectometry is a technique in which a polarized beam of light, operating in two linear polarizations, S and P, optically interrogates a sample. The reflected light from the sample is then measured by a photodetector. Both S and P polarizations, along with the incident angle, are recorded in order to obtain the real component of the refractive index. Equation 3.10 shows how the refractive index of a material is related to the reflection coefficients and angle of incidence.

$$n_R = \sin\theta_i \left[1 + \left(\frac{1-\rho}{1+\rho}\right)^2 \tan^2\theta_i\right]^{\frac{1}{2}} \tag{3.10}$$

Where and $\rho = \sqrt{\frac{R_p}{R_s}}$ and $n_r = \frac{n_2}{n_1}$. Equation 3.10 is used to determine the real part of the refractive index of a material using reflectometry methods [101]. The reflectometer is shown in Fig. 3.19.

2.2) Ellipsometry

Ellipsometry, a closely related technique to reflectometry, can be described with a slight alteration to Equation 3.11. The relative permittivity of a material, , can be found, and is directly related to the refractive index of a material by Equation 3.12 as explained in [102].

$$\langle\tilde{\varepsilon}\rangle = \sin^2\emptyset\left[1+\left(\frac{1-\rho}{1+\rho}\right)^2\tan^2\emptyset\right] \tag{3.11}$$

$$\langle\tilde{\varepsilon}\rangle = n^2 = k \tag{3.12}$$

where $\tilde{\varepsilon}$ and κ are the sample's relative permittivity, n is the refractive index of the sample, ϕ is the incident angle on the sample, and $\rho = \sqrt{\frac{R_p}{R_s}}$ is the ratio of two reflected values for both linear polarizations, P and S. In the system of simple bulk substrate, ellipsometry can determine the refractive index of a material by using the same equation as reflectometry, in albeit formatted. The ellipsometer is shown in Fig. 3.20.

Figure 3.19 Refractometer.

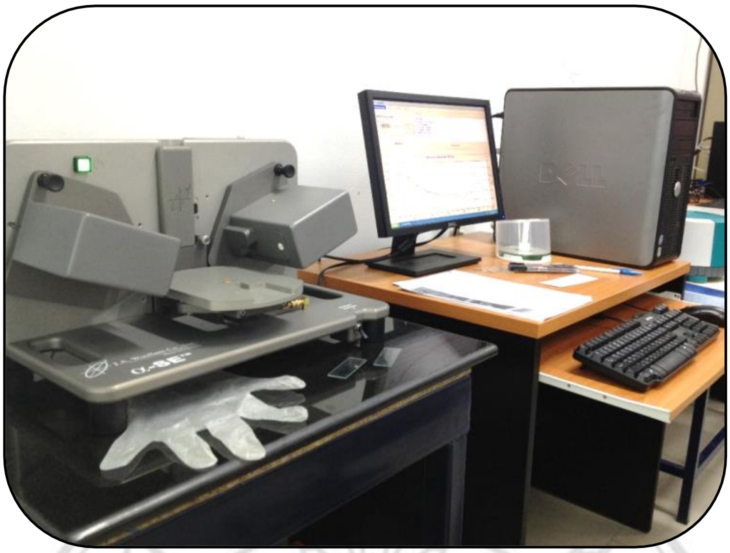

Figure 3.20 Ellipsometer.

However, those methods have some limitations. The limitation of reflectometry is the surface roughness or optical scattering effects which cannot taking into account with this technique. Therefore, the refractive index resulted from reflectometry is a measurement of the optical contributions from both refractive index and surface or substrate roughness. Moreover, reflectometry cannot measure materials that have very highly absorbing layers, because of the completely absorbed.

Ellipsometry also has the same problem when measuring materials that have high absorption for the same reasons. In Addition, this technique also shows other limitation in a case of the unable to estimate thick material, which makes incorrect assumptions or initial guesses in the curve fitting program to determine refractive index and layer thickness.

To prepare sample for measuring refractive index, glass and glass-ceramics with 1 mm in thickness were polished to mirror-like surface by alumina polisher. The well prepared samples must beware of any finger print.

3) Photoluminescence

Photoluminescence (or PL) is the emission of light from any form of material after the absorption of photons. This is called luminescence which was initiated by photoexcitation (excitation by photons). After excitation with photon, the typical relaxation was appeared in which other photons are re-radiated. Time periods between absorption and emission are varied from short femtosecond-regime to milliseconds depending on the types of materials. For examples, for emission involving free-carrier plasma in inorganic semiconductors has very short time period of femtosecond, while phosphorescent processes in molecular systems has longer time period of milliseconds. Moreover, under special circumstances delay of emission may even span to minutes or hours.

Observation of photoluminescence at a certain energy involved the excitation populated an excited state associated with this transition energy. Figure 3.21 and 3.22, the fluorescence spectrometer was adjusted by using 2 excitation sources for different energy conversion response (Hg-lamp source of 310-415 nm for down conversion measurement and laser emitting diode of 980 nm for up conversion measurement). Glass and glass-ceramics with 1 mm. in thickness were polished to mirror-like surfaces and avoided lipid from finger print. The samples were placed on black opaque substrate to reduce the light scattering lose.

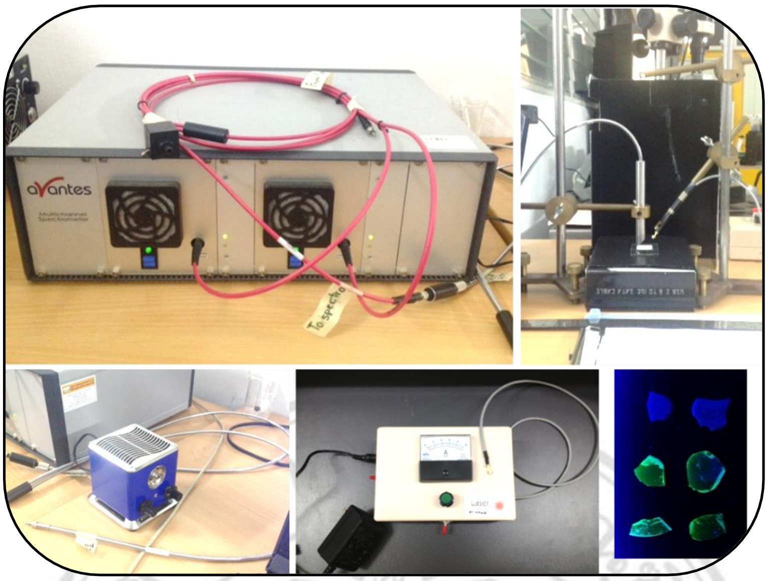

Figure 3.21 Fluorescence spectrometer.

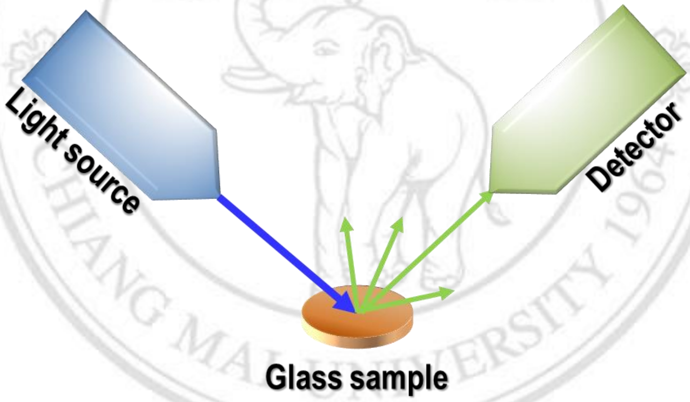

Figure 3.22 Schematic diagram of fluorescence spectrometer adjustment.

3.3.6 Electrical measurement

To study the dielectric property of glass and glass-ceramics in this work, glass and glass-ceramics with 1-2 mm thickness were polished and coated with gold or platinum as an electrode by sputtering technique. Due to the rectangular shape of glass sample, the samples were coated in 2 side, first side is full coat and other side is square coat with dimension of 1x1 mm as shown in Fig. 3.23. The dielectric property was carried out by using LCZ meter (Fig. 3.24) at room temperature and high temperature with frequency in range of

20 Hz to 2 MHz. The relative dielectric constant (ε_r) was calculated from the geometry of the sample and the capacitance [103].

$$\varepsilon = \frac{C \times s}{\varepsilon_0 \times A} \tag{3.13}$$

Where C is the capacitance of the bulk sample,

s is the thickness of the sample,

A is the area of the sample and

ε_0 is free-space permittivity which value of 8.86×10^{-12} F/m.

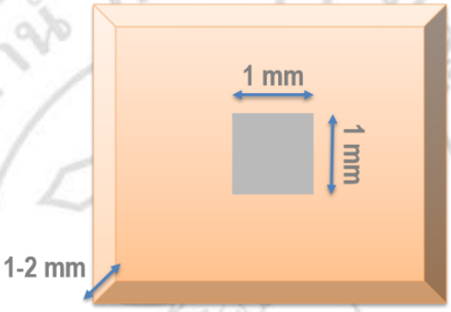

Figure 3.23 Coating electrode in irregular shape sample.

Figure 3.24 LCZ meter.